Inorganic Chemistry

Article

pubs.acs.org/IC

White Phosphorus Degradation with a NacNac Aluminum Carbene Analogue: The Biradical Reaction Mechanism

Wolfgang W. Schoeller*[,†,‡] and Guido D. Frey[‡]

[†]Department of Chemistry, University of California at Riverside, Riverside, California 92521-0403, United States

[‡]Faculty of Chemistry, University of Bielefeld, 33615 Bielefeld, Germany

Supporting Information

ABSTRACT: The title compound Al-NacNac is isolobal to the imidazol-2-ylidene (NHC); the latter is considered as a nucleophilic carbene. However, the title compound is different from a typical carbene, as aluminum is a heavier group 13 element with a predominant inert s orbital. Its singlet ground state is a poor Lewis donor (acceptor) toward white phosphorus, but its corresponding lowest energy triplet state forms a strong Al−P bond with (opened) white phosphorus. The reaction of Al-NacNac with white phosphorus proceeds in two steps: after the addition of a first carbene analogue, a second one is added, resulting in a transient biradicaloid species. This undergoes facile subsequent rearrangement, and a final ring closure reaction leads to the observed product with a bicyclobutane moiety. It is determined by intramolecular bond formation of two phosphorus centered radicals. Finally, a structure with a large singlet−triplet energy separation is formed. An analogy to the noninnocent ligand character as well as the exciplex view of the monoadduct of white phosphorus with the Al-NacNac system is drawn.

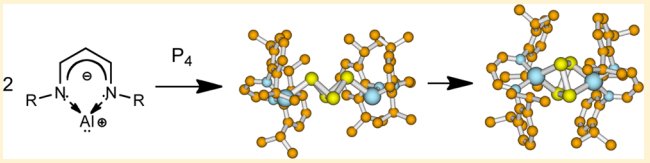

INTRODUCTION

The prolific experimental work of the groups of Roesky and Power paved the way to the syntheses of neutral carbene analogues **1** with the heavier group 13 elements (E = Al,[1,2] Ga,[3] In[4−7] (R = Dipp, R′ = Me, *t*-Bu)), as well as **2** (E = Ga, R = Dipp, R′ = Giso;[8] In (R = Dipp, R′ = Pipiso))[9] (Scheme 1).

Scheme 1

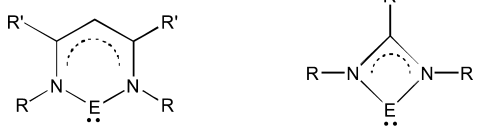

1 **2**

Meanwhile the field of organic aluminum chemistry is rapidly expanding, and a summary of investigations over the last 20 years has been published recently.[10]

The neutral carbene homologue **1** (E = Al) reveals interesting features with respect to its reaction with white phosphorus, P_4[11] (Scheme 2).

Treatment of two equivalents of **1** (E = Al) with white phosphorus at room temperature leads exclusively to **3**. When the reaction was carried out in a **1**:P_4 ratio of 1:1 again, only **3** and some byproducts were obtained. A butterfly structure, **4**, in which one carbene analogue **1** inserts first, and in a second step reacts to **3**, could not be observed. This indicates that the pathway to **3** is either unique or the second insertion process is faster than the first one.

Scheme 2

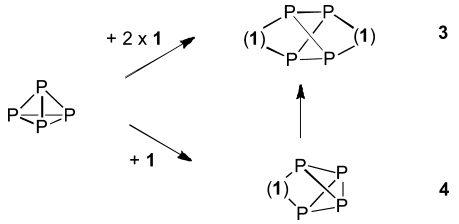

In this report, we present a new perspective on the reaction mechanism for the white phosphorus degradation. It will be shown that the reaction of **1** with P_4 does not follow the insertion mechanism, as it is known for the reaction of silylenes and singlet carbenes with P_4.[12,13] Instead, the P_4 tetrahedron is simultaneously coordinated by two molecules **1**, causing ring-opening without any energy barrier to a biradicaloid species. The latter is then ready for facile subsequent rearrangements, ending finally in an energetic sink **3**. Consequently, **1** acts overall differently than substantiated previously[12,13] for carbenes and silylenes.

RESULTS AND DISCUSSION

a. Qualitative Considerations. Since aluminum is fairly electropositive[14] and the singlet−triplet (S−T) energy separation in **1** is much less than those of typical nucleophilic carbenes (e.g., Arduengo-type NHCs,[15,16] in which the S−T energy separation for the parent system is 79.4 kcal/mol[17]), **1**

Received: October 30, 2013
Published: May 6, 2014

dx.doi.org/10.1021/ic402649b | Inorg. Chem. 2014, 53, 4840−4846

reveals a lower S−T energy separation (R = terphenyl 21.7, Me 28.4; phenyl, mesityl, and dipp 28 to 31 kcal/mol; R′ = H).[18] On this basis, **1** is expected to react as a nucleophilic as well as an electrophilic carbene homologues species. The carbene character is based on the fact that **1** is best described in the singlet state as a chelate complex of an Al cation in the oxidation state +I ($^1s^2$ configuration at Al), as depicted in **1 (S)** (Scheme 3).

Scheme 3

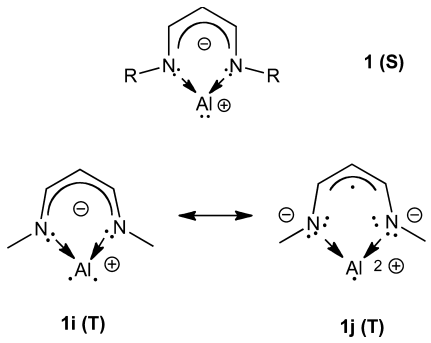

In comparison, the corresponding triplet state is best grasped by two canonical structures **1i (T)** and **1j (T)**. The first one ($^3s^1p^1$) refers again to the Al cation in the formal oxidation state +I, while in the latter, one electron of the Al is distributed over the allylic system of the NacNac ligand and the formal oxidation state of the metal is +II. This gives rise to unique donor−acceptor formation.[19] Hence the NacNac-ligand becomes noninnocent with regard to a change from the singlet to the triplet state in **1**. In the latter state, the central metal atom aluminum can easily change its oxidation state from +I to +II. One consequence of this aspect has already been explored, the triplet can be strongly stabilized by radical stabilizing substituents at the ligand system.[19] A further consequence, the facile electronic coupling of two triplet fragments of **1** toward an opened white phosphorus will be evaluated here. It gives rise to biradicaloid formation with subsequent easy formation of the formal double-insertion product **4**.

For the reaction of **1** with white phosphorus, it is mandatory to briefly consider the molecular orbital system of P_4. Symmetry considerations[12,13] give support to the following qualitative model (Scheme 4).

(a) The four corners of the tetrahedron supply lone pairs at phosphorus. These are the preferred positions for an attack of an electrophile El (approach path i). (b) Nucleophilic species (Nu) add preferentially tangentially to the corners of the tetrahedron (approach path k). (c) A third approach, path j, can be envisioned, the direct insertion of an electrophile into one of the P−P bonds. Carbenes or silylenes, depending on their prevailing electrophilic or nucleophilic character, react with white phosphorus in consecutive steps (1 carbene/silylene:1 P_4) either to **4** (electrophilic carbene/silylene)[20,21] or immediate ring-opening (nucleophilic carbene).[22−24] Consecutively, a second carbene/silylene is added.

Scheme 4

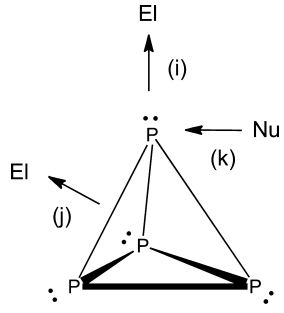

One further aspect must be taken into consideration. To break one P−P bond of the P_4 tetrahedron is estimated to result in 51 kcal/mol in energy,[25,26] while the bond energy of a formed AlP bond is less than this value. An estimate of 47 kcal/mol for the dissociation of an AP bond ($^3\Sigma^-$) was obtained from quantum chemical investigations.[27] This makes an insertion process of only one aluminum carbene homologue **1** into P_4 via a direct insertion process unlikely. In the following discussion, a biradical pathway will be evaluated; an unusual reaction behavior of **1**, it is a consequence of the noninnocent ligand system within the lowest energy triplet state.

b. The Biradical Pathway. For convenience, the reaction of **1** was first studied in detail with the substituents R = Me and R′ = H, in order to explore the facets of the different reaction paths. However, in the experiment, **1** is substituted by sterically encumbering substituents (e.g., R = Dipp (2,6-diisopropylphenyl)), in order to protect it from competing side reactions. These steric effects will be discussed in a later section of the publication, but their consideration is not required to reveal the overall reaction mechanism.

The process is initiated by reaction 1, which refers to the formation of **5**, a weak adduct of **1** with white phosphorus P_4. An inspection of the molecular orbitals identifies **5** as a weak donor−acceptor complex, in which P_4 acts as a weak donor and **1** as a weak acceptor.

$$\mathbf{1} + P_4 \rightarrow \mathbf{1}{-}P_4 \quad (1)$$

$$\mathbf{1}{-}P_4 + \mathbf{1} \rightarrow \mathbf{1}{-}P_4 - \mathbf{1} \quad (2)$$

An analysis of the electron distribution results for the singlet **5(S)** less than a single bond (AlP = 2.789 Å, SEN (shared electron number of bonds) = 0.597), which is essentially stronger in the lowest energy triplet **5(T)** (AlP = 2.433 Å, SEN = 1.129). For the former, **5(S)**, the association energy, reaction 1, results in ΔE = −9.4 kcal/mol (ΔG (298 K, p = 1 atm) = 1.9 kcal/mol). A corresponding reaction 1 for the formation of a triplet from **1(T)** and **P_4(T)** yields a PAl-bond energy of ΔE = −70.5 kcal/mol, much larger than that for the singlet. The equilibrium geometries of lowest energy singlet and triplet states of **5** are recorded in Figure 1 (top). There is a noticeable difference between both structures. In the singlet adduct, the P_4 tetrahedron remains intact, while in the triplet one PP bond is already broken. For **5** still the singlet prevails as the ground state, but according to the density-functional calculations the adiabatic singlet−triplet (S−T) energy separation is fairly small (ΔE(S−T) = −17.2 kcal/mol).

For the further discussion, it is important to inspect the spin density distributions within **5(T)**. [In the following discussion, (S) abbreviates as singlet and (T) as triplet]. The spin densities are summarized in Figure 1 (bottom). A strong localization of spin densities is observed at aluminum (0.703 el) and its neighboring (0.267 el) as well its distal (0.822 el) suited phosphorus atoms.

The population analysis indicates no further substantial spin delocalization (<0.01 el) at the other phosphorus atoms and/or at the other atoms of the [LAl] fragment. Thus, bonding in

dx.doi.org/10.1021/ic402649b | Inorg. Chem. 2014, 53, 4840−4846

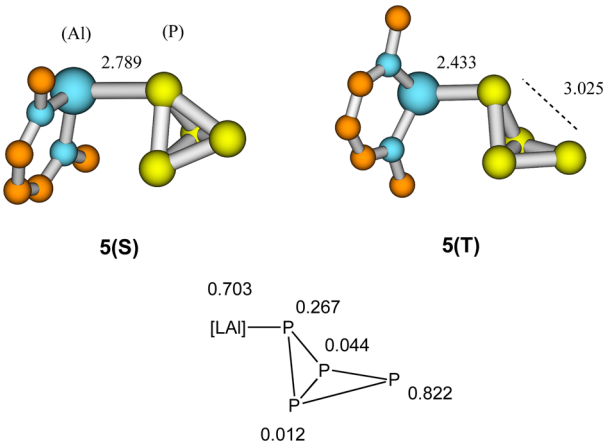

Figure 1. Equilibrium geometries of singlet **5(S)** and triplet **5(T)** monoadducts of [LAl] (= **1**, R = Me, R′ = H) with P_4 (bond lengths are in Ångstroms units) and spin densities of **5(T)** (NBO-population analysis). For convenience hydrogens are omitted.

5(T) can be grasped in two canonical structures, **5i** versus **5j** (Scheme 5).

Scheme 5

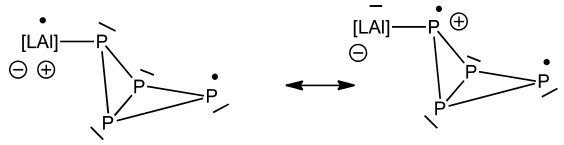

In **5i**, spin density is located preferentially at the metal and the distal phosphorus atom, while in **5j** the unpaired density resides at the distal phosphorus centers.

The overall bonding situation, the adduct **5** fairly weakly bonded in a singlet ground state, but stronger bonding in an excited state (triplet) is reminiscent of an excited state complex (exciplex), as these are well established in photochemistry and in the redox chemistry with transition metals.[28] One may note also that superweak complexes of tetrahedral P_4 with silver cations could be structurally characterized.[29]

The presented detailed analysis on **5(T)** is of importance for rating its further reactivity. The species can add a second unit **1**, as it is described in reaction 2, thus forming a structural unit **6**. The opened P_4 is here flanked by two carbene homologues. More structural details of **6(S)** are given in Figure 2. Reaction 2 is more strongly exothermic ($\Delta E = -21.5$, $\Delta G = 8.4$ kcal/mol) than the first addition step, i.e. reaction 1. Species **6** adopts a butterfly conformation and takes up a biradical structure with a singlet ground state (ΔE(S−T) = −1.7 kcal/mol). Reaction 2 is even more exothermic than reaction 1. It is the consequence of the already enforced butterfly structure by interaction of one [LAl] (= **1**, R = Me) with the P_4 moiety, i.e., the formation of **5(T)**. Alternatively, **6** can be viewed as the diamagnetic (**S**) or paramagnetic (**T**) coupling of two triplets[30] over the central PP bridge. The latter exerts weak π-character.[31] More details, equilibrium geometries of the investigated species and full details of the spin densities of **5(T)** and **6(T)**, are collected in the Supporting Information of this publication.

Biradicaloids are in general highly unstable species. Thus, it is logical to assume that the singlet biradical **6** undergoes facile rearrangement reactions. All of the geometrical structures, which could be traced by the quantum chemical investigations, are summarized in Figure 2. The various intermediates rest in shallow energy minima and are separated by small energy barriers. They were determined by energy minimization subjected to vibrational analyses; corresponding transition states were evaluated by detailed surface scans interconnecting the various energy minima. A schematic representation of the cascade mechanism is given in Figure 3. Free energies (ΔG(rel), T = 298 K, p = 1 atm, values in parentheses, in kcal/mol) are in reference to singlet **6**. In addition, all equilibrium geometries of the singlet hypersurface are collected in the Supporting Information. Solid lines in Figure 3 pronounce the backbone P_4 framework.

All of the investigated structures prefer singlet ground states. It is informative to have knowledge of the adiabatic singlet−triplet (ΔE(S−T)) energy differences. These are added in brackets to the relative energies (values are in kcal/mol). Structure **6** is the starting point for the reaction cascade over the various intermediates. It is a highly unstable biradical and thus amenable to an easy rearrangement. Overall the reaction cascade is dictated by (a) a low energy barrier for rearrangement, (b) a drop in energy for the resulting structural intermediates, and (c) finally a suitable reordering of the arrays of the phosphorus atoms, such as to allow a PP-bond formation to the final product. For convenience, the phosphorus atoms in Figure 3 are labeled with Greek letters and the metal atoms with Roman letters.

A first step is the migration of one [AlL] fragment from P(α) to P(β) (Figure 3). It causes the formation of (singlet) **7**. With migration of Al(a) toward P(β) the bond P(β)P(α') becomes at the same time unstable and breaks. The energy barrier for this process is 3.7 kcal/mol and results for **7** in an energy drop of −25.9 kcal/mol. An inspection of the equilibrium geometry (Figure 2) evidences a phosphino-tricyclophosphene frame with two complexing [AlL] fragments. Even though **7** reveals a pronounced closed-shell character [$-\Delta E$(S−T) = 25.4 kcal/mol], it is unstable toward further rearrangement to **8**. The latter is considerably more stable than the former structure, yet it has only a smaller preference for the singlet state ($-\Delta E$(S−T) = 2.6 kcal/mol). The drop in energy from **7** to **8** is due to the additional gain of an AlP bond (see vide infra); the reaction requires only a rotation at the bond P(α')P(β').

In the final product **11**, the PP bonds are rearranged; e.g., P(α) links with P(α') and P(β). It requires that the bond P(α)P(β') has to be broken. It can be done by following a cascade mechanism **8** → **9** → **10** → **11**. Structure **10** is again biradical in nature [$-\Delta E$(S−T) = 0.5 kcal/mol] and closes readily to the final product **11**. The reordering of the backbone bonds is accompanied by a corresponding shift of the [AlL] fragment. Interestingly, a detailed inspection of the electronic hypersurface by corresponding scans did not trace a low-energy path for direct bond formation between Al(a) and P(β') in **8**, which could lead to **10**. Rather the pathway over the intermediate **9** is preferred.

Some questions appear fundamental in the present discussion, (a) what determines the various relative energetic stabilities in reference to biradical **6** and (b) why is the energy difference between singlet and triplet in the various intermediate species different? A hint to the first point is given by an inspection of the equilibrium geometries collected in Figure 2. Throughout, in all structures the AlP-bond distances range between 2.4 and 2.5 Å, comparable to the AlP

dx.doi.org/10.1021/ic402649b | Inorg. Chem. 2014, 53, 4840−4846

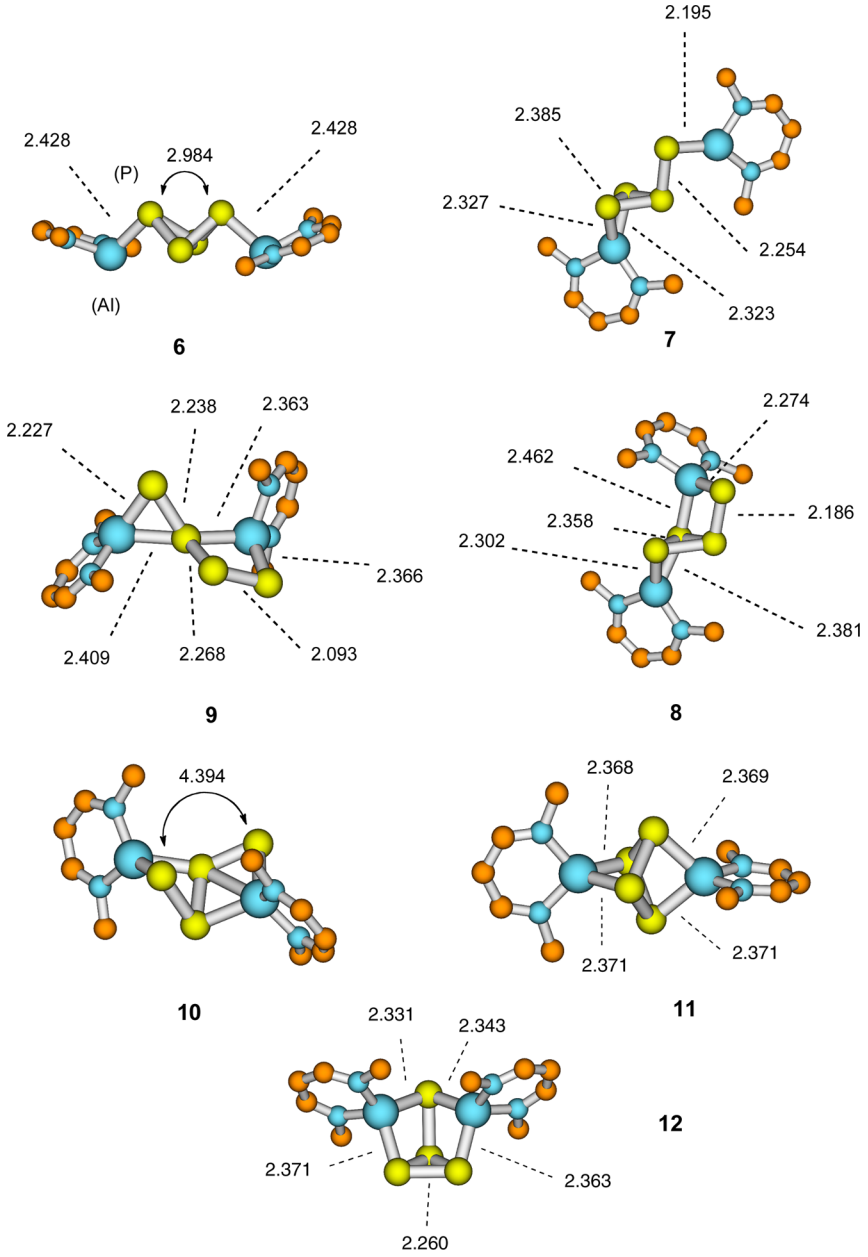

Figure 2. Plots of the equilibrium geometries of the model compounds **6** to **11** in their lowest energy singlet states. For clarity, the hydrogens are omitted. Relevant bond distances are in Ångstrom units.

bond in **5(T)** (2.433 Å) but essentially shorter than in **5(S)** (2.789 Å). It indicates that the AlP bonds in the intermediates **6** to **10** and also in **11** are rather strong. The structure **6** has only two AlP bonds; it is the least stable species on the hypersurface, while **7** bears three and **8** to **11** four AlP bonds. On this basis, the last species represent the energetic sink on the electronic hypersurface.

The singlet−triplet energy separation can be estimated by valence-bond-Lewis (VBL) structure diagrams. These will be drawn for **7** and **10**. Structure **7** is fairly stable ($-\Delta E$(S−T) = 25.4 kcal/mol). As indicated in **7i**, a perfect pairing of two triplet units [AlL] with the phosphorus backbone system is achieved (Scheme 6).

The smallest ΔE(S−T) is obtained from the DFT calculations for **6** and **10**. It refers to cases in which the terminal phosphorus atoms of the phosphorus chain are linked to a central PP bridge. For **10**, a corresponding VBL diagram (Scheme 7) makes a phosphorus centered biradical structure **10i** apparent.

The P_4 fragment is here considered as two phosphinidenes, each in triplet state, interacting with two triplet [AL] molecules. It emerges into a biradical with unpaired electron density preferentially located at two phosphorus atoms. It is in contrast to **6** with unpaired electron density spread over the aluminum and their linked phosphorus atoms.

The present DFT calculations cannot predict the localization of unpaired electron density. However, the analysis of the triplet state, which adopts an almost identical equilibrium geometry as the biradical singlet and results in a fairly small S−T energy separation to the singlet, indicates a spin distribution in accord with **10i** (for details see the Supporting Information). On this basis, one expects that the biradical singlet of **10** is facile for intramolecular PP-bond formation to the final product **11**.

dx.doi.org/10.1021/ic402649b | *Inorg. Chem.* 2014, 53, 4840−4846

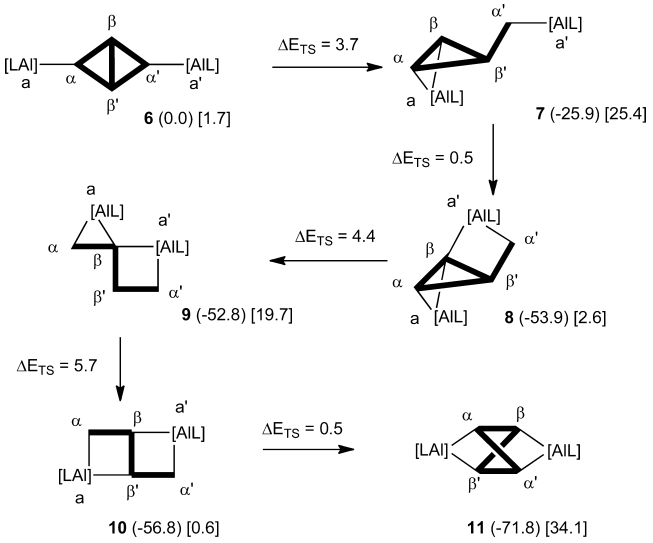

Figure 3. Schematic reaction cascade of biradicaloid **6** over the various unstable intermediates to the final product **11**. Relative free energies (parentheses, in kcal/mol) are in reference to the bis-adduct **6**. Solid lines indicate the P_4 framework, [AlL] = **1** (R = Me, R′ = H); ΔE(TS) refers to transition state energies (in parentheses), in brackets are adiabatic $-\Delta E$(S−T) energies of intermediates.

Scheme 6

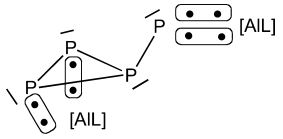

7i

Scheme 7

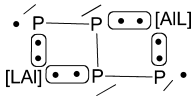

10i

In our investigations we found a further energy minimum **12**. It is even slightly more stable (ΔG(rel) = −73.0, ΔE(S−T)= 29.9) kcal/mol) than **11** (ΔG(rel) = −71.8, $-\Delta E$(S−T) = 34.1), but it has not been found in the experiment. The VBL treatment also predicts for **12** a perfect pairing of the electrons. It agrees with the outcome of the calculations, which yield a large S−T energy separation for **12**. In the experiment, however, only **11** is observed. We explain this by the facile ring closure reaction of **10** to the experimental outcome.

The discussion outlined on the relative stabilities of **6** to **12** is based on relative free energies of the singlet structures of the investigated species. We have subjected all stationary energy minimum structures to vibrational analysis and evaluated corresponding entropy contributions. Since the rearrangement from **6** to **11** refers to a sequence of monomolecular reactions, the entropy corrections are fairly similar and relative energy ΔE values and ΔG values parallel each other. A full list of all energy values is collected in the Supporting Information of this publication.

To reveal the role of steric effects on the biradicaloid intermediates we also performed calculations for the reaction of **1** (R = Dipp, R′ = H) with P_4, in order to mimic fully the experimental situation. The outcome for the reaction hypersurface is fairly similar to the model case with R = H. The only difference is the larger exothermicity (ΔG = −108 kcal/mol) upon formation of **11-Dipp** from **6-Dipp**. Previous considerations have enforced a similarity between a Me- and a Dipp-substituent, since the latter refers to its steric demand for an oblique cone.[32] A full record of the studied intermediate structures (equilibrium structures, relative and free energies) for R = Dipp, R′ = H is given in the Supporting Information.

A further question is that to the role of possible solvation effects on the rearrangement reaction. We have probed this for the Dipp-substituted intermediates. Assuming a solvent with a small dielectric constant (μ = 1.75, tetrahydrofuran), the effect on the stabilization on each intermediate structure is fairly similar. It amounts to ca. 4−5 kcal/mol for stabilization energy of each species. Thus, the overall cascade mechanism is not altered. A detailed listing of the resulting energies is collected in the Supporting Information.

c. Insertion of a Single Al-NacNac Compound. The present investigations reveal the facile insertion reaction of two pseudocarbenes **1**. The outlined mechanism reveals no energy barrier for the insertion process, in agreement with the reported experimental conditions.[11] Can only one species **1** insert into the P_4 tetrahedron? A corresponding reaction path was computationally studied as well, it is summarized in the following energy diagram (Figure 4).

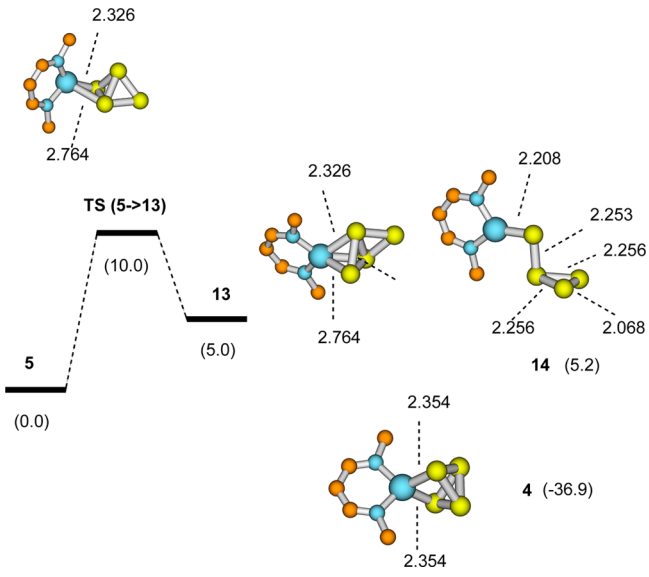

Figure 4. Energy diagram for the reaction path for a single **1** (R = Me, R′ = H) into the P_4 tetrahedron. Values refer to relative free energies (298 K, 1 atm) in kcal/mol, at times in reference to singlet **6**, bonding parameters are in Ångstrom units.

In the transition state one PP bond of the P_4 tetrahedron is already broken, and simultanously a partial neighboring AlP bond is formed. In other words, partial AlP-bond formation assists the reaction process. The transition state is higher in energy than the (singlet) educt **5**. It leads to an intermediate species **13**; its dipolaric nature is substantiated by a population analysis. Further, **13** adds one species **1**; it forms the intermediate **8** without any energy barrier. The latter is part of the reaction cascade (Figures 2, 3). Thus, a two-step process with an energy barrier is revealed, while the biradical pathway proceeds without any energy barrier. Figure 4 records

dx.doi.org/10.1021/ic402649b | Inorg. Chem. 2014, 53, 4840−4846

additional structural isomers of **13**. Structure **14** refers to a triphospha-cyclopropene derivative. Although it appears as an energy minimum on the hypersurface, it rearranges easily to the most stable species, the monoinsertion product **4**. It possesses a singlet structure with a sizable S−T energy separation.

COMPUTATIONAL DETAILS

All calculations were performed with the Gaussian 09[33] and Turbomole 6.2[34] set of programs. Density Functional Theory (DFT) was employed throughout. The structures were optimized without any symmetry constraints at the BP86 level,[35] at times supplemented by dispersion correction terms.[36] In all cases, the RI ("resolution of the identity") approximation[37] was imposed. As a basis set, the TZVP was chosen.[38] Frequency calculations were performed numerically for the bulky structures and analytically for the small (model) structures; entropies and free energies were determined by standard equations from statistical thermodynamics.[39] The structures with small S−T energy separations were tested against spin contamination, eventually reoptimized at singlet UHF level and, when necessary, energy corrected within the broken-symmetry approach.[40] The population analyses (details are not listed here) were conducted within the electron density partitioning scheme of Ahlrichs and Ehrhardt and of Mayer.[41,42]

CONCLUSIONS

The results of our investigations can be summarized as follows:

(1) The Al(NacNac) compound **1** can be considered as a formal analogue to a singlet carbene. However, there is a difference: the HOMO lone pair orbital in the singlet state ($^1s^2$ configuration at Al) is an inert s orbital, since aluminum is a heavier main group element.

(2) Thus, a singlet donor−acceptor complex with white phosphorus is rather weak with regard to dissociation into two fragments. It is different in the triplet state ($^3s^1p^1$ at aluminum). One electron of the inert s orbital is promoted to a valence p orbital, which is more suitable for bond formation. As a consequence the Al−P bond for adduct formation is shorter, and the resulting S−T energy separation in the complex becomes less than in the free carbene analogue. An analogous bonding behavior via an exciplex formation (stronger donor−acceptor bond in an excited state) can be evoked, due to the formal change of the oxidation state in Al to +II in the triplet. It gives rise to consecutive addition of a biradicaloid species without an energy barrier. On this basis the carbene analogue **1** can also be viewed as a noninnocent ligand system,[19] due to a change in the oxidation state of the metal by adding the P_4 fragment as a further ligand.

(3) The electronic coupling of a triplet **1** with P_4 can be rated on the basis of valence bond Lewis (VBL) diagrams. In accord with the calculations the addition of two molecules of **1** to P_4 forms a biradicaloid species, which is facile to further subsequent migration of the [AlL] fragments over the P_4 moiety. The final product is determined by perfect pairing of the two triplet fragments with the phosphorus ring system.

(4) The energy sink is overall the double-insertion product **11**. It is kinetically favored over **12**, since intramolecular radical−radical combination facilitates the former species.

Our investigations reveal a new facet in aluminum chemistry; biradicaloids are formed, amenable to easy rearrangement processes. How far this can be attributed to reactions of other processes, such as the addition to sulfur, remains to be established. This is currently under investigation.

ASSOCIATED CONTENT

Supporting Information

Equilibrium geometries of the investigated species and full details of the spin densities of **5(T)** and **6(T)**. This material is available free of charge via the Internet at http://pubs.acs.org.

AUTHOR INFORMATION

Corresponding Author

*E-mail: wolfgang.schoeller@uni-bielefeld.de.

Notes

The authors declare no competing financial interest.

ACKNOWLEDGMENTS

We thank the Department of Chemistry at the University of Bielefeld (Germany) and the University of California Riverside (USA) for allocation of computer time, Dr. T. Tönsing for computational assistance, and Dr. R. D. Dewhurst for helpful discussions. We also thank the Deutsche Forschungsgemeinschaft for support in an earlier stage of this research.

DEDICATION

Dedicated to Richard Otto

REFERENCES

(1) Cui, C.; Roesky, H. W.; Schmidt, H.-G.; Noltemeyer, M.; Hao, H.; Cimpoesu, F. *Angew. Chem., Int. Ed.* **2000**, *39*, 4274−4276.
(2) Li, X.; Cheng, X.; Song, H.; Cui, C. *Organometallics* **2007**, *26*, 1039−1043.
(3) Hardman, N. J.; Eichler, B. E.; Power, P. P. *Chem. Commun.* **2000**, 1991−1992.
(4) Stender, M.; Power, P. P. *Polyhedron* **2002**, *21*, 525−529.
(5) Hill, M. S.; Hitchcock, P. B. *Chem. Commun.* **2004**, 1818−1819.
(6) Hill, M. S.; Hitchcock, P. B.; Pontavornpinyo, R. *Angew. Chem., Int. Ed.* **2005**, *44*, 4231−4235.
(7) Hill, M. S.; Hitchcock, P. B.; Pontavornpinyo, R. *Dalton Trans.* **2007**, 731−733.
(8) Jones, C.; Junk, P. C.; Platts, J. A.; Stasch, A. *J. Am. Chem. Soc.* **2006**, *128*, 2206−2207.
(9) Jones, C.; Junk, P. C.; Stasch, A.; Woodul, W. D. *New J. Chem.* **2008**, *32*, 835−842.
(10) Asay, M.; Jones, C.; Driess, M. *Chem. Rev.* **2011**, *111*, 354−396.
(11) Peng, Y.; Fan, H.; Zhu, H.; Roesky, H. W.; Magull, J.; Hughes, C. E. *Angew. Chem., Int. Ed.* **2004**, *43*, 3443−3445.
(12) Schoeller, W. W. *Phys. Chem. Chem. Phys.* **2009**, *11*, 5273−5280.
(13) Schoeller, W. W. *Theor. Chem. Acc.* **2010**, *127*, 223−229.
(14) Pauling, L. *The Nature of the Chemical Bond and the Structure of Molecules and Crystals*; Cornell University Press: Ithaca, NY, 1960.
(15) Arduengo, A. J.; Harlow, R. L.; Kline, M. *J. Am. Chem. Soc.* **1991**, *113*, 361−363.
(16) Öfele, K.; Herberhold, M. *Angew. Chem., Int. Ed. Engl.* **1970**, *9*, 739−740.
(17) Dixon, D. A.; Arduengo, A. J., III. *J. Phys. Chem.* **1991**, *95*, 4180−4182.
(18) Schoeller, W. W. *Inorg. Chem.* **2011**, *50*, 2629−2633.
(19) Schoeller, W. W.; Frey, G. D. *J. Organomet. Chem.* **2013**, *744*, 172−177.
(20) Xiong, Y.; Yao, S.; Brym, M.; Driess, M. *Angew. Chem., Int. Ed.* **2007**, *46*, 4511−4513.
(21) Martin, C. D.; Weinstein, C. M.; Moore, C. E.; Rheingold, A. L.; Bertrand, G. *Chem. Commun.* **2013**, *49*, 4486−4488.
(22) Masuda, J. D.; Schoeller, W. W.; Donnadieu, B.; Bertrand, G. *Angew. Chem., Int. Ed.* **2007**, *46*, 7052−7055.
(23) Masuda, J. D.; Schoeller, W. W.; Donnadieu, B.; Bertrand, G. *J. Am. Chem. Soc.* **2007**, *129*, 14180−14181.

(24) In the first step of this process, a triphospha-cyclopropene is formed, which subsequently proceeds over a cascade of intermediates to a final phosphorous cluster.
(25) Pauling, L.; Simonetta, M. *J. Chem. Phys.* **1952**, *20*, 29−34.
(26) Schoeller, W. W.; Staemmler, V.; Rademacher, P.; Niecke, E. *Inorg. Chem.* **1986**, *25*, 4382−4385.
(27) Gan, Z.; Grant, D.; Harrison, R.; Dixon, J. *J. Chem. Phys.* **2006**, *125*, 124311-1−124311-6.
(28) Kuzmin, M. G.; Soboleva, I. V.; Dolotova, E. V. *Adv. Phys. Chem.* **2011**, 1−18.
(29) Krossing, I.; van Wüllen, L. *Chem.—Eur. J.* **2002**, *8*, 700−711.
(30) Trinquier, G. *J. Am. Chem. Soc.* **1990**, *112*, 2130−2137.
(31) Schoeller, W. W.; Lerch, C. *Inorg. Chem.* **1983**, *22*, 2922−2998.
(32) Schoeller, W. W.; Frey, G. D.; Bertrand, G. *Chem.—Eur. J.* **2008**, *14*, 4711−4718.
(33) Frisch, M. J.; Trucks, G. W.; Schlegel, H. B.; Scuseria, G. E.; Robb, M. A.; Cheeseman, J. R.; Scalmani, G.; Barone, V.; Mennucci, B.; Petersson, G. A.; Nakatsuji, H.; Caricato, M.; Li, X.; Hratchian, H. P.; Izmaylov, A. F.; Bloino, J.; Zheng, G.; Sonnenberg, J. L.; Hada, M.; Ehara, M.; Toyota, K.; Fukuda, R.; Hasegawa, J.; Ishida, M.; Nakajima, T.; Honda, Y.; Kitao, O.; Nakai, H.; Vreven, T.; Montgomery, J. A., Jr.; Peralta, J. E.; Ogliaro, F.; Bearpark, M.; Heyd, J. J.; Brothers, E.; Kudin, K. N.; Staroverov, V. N.; Kobayashi, R.; Normand, J.; Raghavachari, K.; Rendell, A.; Burant, J. C.; Iyengar, S. S.; Tomasi, J.; Cossi, M.; Rega, N.; Millam, J. M.; Klene, M.; Knox, J. E.; Cross, J. B.; Bakken, V.; Adamo, C.; Jaramillo, J.; Gomperts, R.; Stratmann, R. E.; Yazyev, O.; Austin, A. J.; Cammi, R.; Pomelli, C.; Ochterski, J. W.; Martin, R. L.; Morokuma, K.; Zakrzewski, V. G.; Voth, G. A.; Salvador, P.; Dannenberg, J. J.; Dapprich, S.; Daniels, A. D.; Farkas, Ö.; Foresman, J. B.; Ortiz, J. V.; Cioslowski, J.; Fox, D. J. *Gaussian 09*, Revision A.1; Gaussian, Inc.: Wallingford CT, 2009.
(34) Turbomole V6.2. http://www.turbomole.com.
(35) (a) Vosko, S. H.; Wilk, L.; Nusair, M. *Can. J. Phys.* **1980**, *58*, 1200−1211. (b) Becke, A. D. *Phys. Rev. A* **1988**, *38*, 3098−3100. (c) Perdew, J. P. *Phys. Rev. B* **1986**, *33*, 8822−8824.
(36) Grimme, S. *J. Comput. Chem.* **2004**, *25*, 1463−1473.
(37) Arnim, M. V.; Ahlrichs, R. *J. Comput. Chem.* **1998**, *19*, 1746−1757.
(38) Schäfer, A.; Huber, C.; Ahlrichs, R. *J. Chem. Phys.* **1994**, *100*, 5829−5835.
(39) McQuarrie, D. A. *Statistical Mechanics*; Harper & Row: New York, 1976.
(40) Yamaguchi, K.; Jensen, F.; Dorigo, A.; Houk, K. N. *Chem. Phys. Lett.* **1988**, *149*, 537−542.
(41) Ehrhardt, C.; Ahlrichs, R. *Theor. Chim. Acta* **1985**, *68*, 231−245.
(42) Mayer, I. *J. Comput. Chem.* **2007**, *28*, 204−221.